Widespread Decrease of Type 1 Cannabinoid Receptor Availability in Huntington Disease In Vivo

Koen Van Laere[1], Cindy Casteels[1], Isabel Dhollander[2], Karolien Goffin[1], Igor Grachev[3], Guy Bormans[4], and Wim Vandenberghe[2]

[1]Division of Nuclear Medicine, Leuven University Hospital and Katholieke Universiteit Leuven, Leuven, Belgium; [2]Department of Neurology, Leuven University Hospital and Katholieke Universiteit Leuven, Leuven, Belgium; [3]Merck & Co., Inc., Imaging Center, West Point, Pennsylvania; and [4]Laboratory of Radiopharmaceutical Chemistry, Katholieke Universiteit Leuven, Leuven, Belgium

The type 1 cannabinoid receptor (CB1) is a crucial modulator of synaptic transmission in the brain. Animal and postmortem human data suggest that mutant huntingtin represses CB1 transcription. Our aim was to measure CB1 levels in the brains of Huntington disease (HD) patients in vivo. **Methods:** Twenty symptomatic HD patients and 14 healthy controls underwent PET with the novel CB1 ligand N-[2-(3-cyano-phenyl)-3-(4-(2-^{18}F-fluoroethoxy)phenyl)-1-methylpropyl]-2-(5-methyl-2-pyridyloxy)-2-methylproponamide. **Results:** We observed a profound decrease of CB1 availability throughout the gray matter of the cerebrum, cerebellum, and brain stem in HD patients, even in early disease stages. Disease burden ([number of CAG repeats in the *HTT* gene – 35.5] × age) was inversely correlated with CB1 availability in the prefrontal and premotor cortex. **Conclusion:** The profound early and widespread reduction of CB1 availability in vivo is consistent with the hypothesis that mutant huntingtin represses CB1 transcription. This is the first, to our knowledge, in vivo demonstration of disturbance of the endocannabinoid system in a human neurologic disease.

The type 1 cannabinoid receptor (CB1) is a key modulator of synaptic transmission in the mammalian brain. CB1 is abundantly expressed on presynaptic terminals, where its activation suppresses neurotransmitter release (*1*). CB1 can be activated by Δ^9-tetrahydrocannabinol, the active ingredient of marijuana, but also by endogenous agonists (endocannabinoids). CB1 signaling is involved in the physiologic regulation of motor behavior, cognition, emotion, and food intake and also in pathologic processes in animal models of movement disorders (*2*) and addiction (*3*). Whether disturbances of the endocannabinoid system (ECS) also play a role in neurologic diseases in humans remains more speculative.

Huntington disease (HD) is a dominantly inherited neurodegenerative disease manifested by motor, cognitive, and psychiatric dysfunction (*4*). Neuroimaging and pathologic studies indicate that neurodegeneration in HD is regionally selective and preferentially affects the striatum and cerebral cortex, whereas other brain areas remain largely spared until advanced disease stages (*5,6*). HD is caused by expansion of a number (n) of CAG repeats in the *HTT* gene ([CAG]$_n$), leading to an expanded polyglutamine tract in huntingtin, a protein with unknown function and abundant, ubiquitous expression in the brain. Accumulating evidence suggests that the expanded polyglutamine tract leads to aberrant interactions between mutant huntingtin and nuclear transcription factors, thereby disturbing the transcription of a subset of genes (*7*). Several transcriptionally active drugs ameliorate the HD phenotype in preclinical trials, further supporting a role for transcriptional dysregulation in HD pathogenesis (*8*). Interestingly, CB1 messenger RNA (mRNA) is one of the most consistently decreased transcripts in postmortem striatal tissue from a range of transgenic HD mouse models and HD patients (*9*). Furthermore, a loss of CB1 protein was demonstrated in the basal ganglia of deceased HD patients (*10*). Whether CB1 levels are changed in HD brains in vivo is unknown.

In vivo imaging of CB1 in the human brain has recently become feasible using quantitative PET with the highly selective, high-affinity CB1 radioligand N-[2-(3-cyano-phenyl)-3-(4-(2-^{18}F-fluoroethoxy)phenyl)-1-methylpropyl]-2-(5-methyl-2-pyridyloxy)-2-methylproponamide (^{18}F-MK-9470) (*11*). The aim of the present study was to investigate CB1 availability in the brains of HD patients in vivo.

MATERIALS AND METHODS

Subjects

We recruited 20 patients with symptomatic HD and 14 age- and sex-matched healthy controls. The study was approved by the institutional Ethics Committee and performed in accordance with the World Medical Association Declaration of Helsinki. Written informed consent was obtained from all subjects or their legal representatives before the study.

Patients with past or current alcohol or drug abuse were excluded. All HD patients were symptomatic, as defined by the presence of visible chorea, and had a $(CAG)_n$ of at least 39. The Unified Huntington's Disease Rating Scale (UHDRS) motor and total functional capacity (TFC) scores (12) were obtained on or around the day of PET (mean interval, 0.5 d; range, −58 to +27 d). The HD study population covered the entire spectrum of symptomatic disease severity (Table 1).

In total, 50 healthy controls between 18 and 70 y were recruited prospectively for different ongoing studies. Age- and sex-matching was performed in this study because a previous ^{18}F-MK-9470 PET study in healthy controls showed significant variation of CB1 mapping with age and sex (13). To also match body mass index, the 2 volunteers with the highest body mass index were excluded, and the other 14 age-matched controls were retained. Inclusion and exclusion criteria for controls were as previously described (13).

All subjects in this study underwent physical examination and blood and urine testing to exclude major internal pathology. Urine toxicology for cannabis and all major known addictive drugs was performed (13); only nonsmokers (for at least 6 mo) were included.

Methods of radiotracer preparation, imaging, image processing, data analysis, and analysis design are described in the supplemental materials (available online only at http://jnm.snmjournals.org).

RESULTS

Patient Characteristics

Patient demographics and disease characteristics are summarized in Table 1. Seven HD patients were in Shoulson–Fahn stage I and thus represented the earliest phase of symptomatic disease. The number of (CAG) repeats correlated strongly with age at the time of study ($r = −0.81$, $P = 2 \cdot 10^{-5}$) and age at symptom onset ($r = −0.90$, $P = 2 \cdot 10^{-7}$). The TFC score correlated with motor score ($r = −0.86$; $P = 1 \cdot 10^{-6}$) and disease duration ($r = −0.77$, $P = 7 \cdot 10^{-5}$).

MRI

As expected, we detected substantial reductions of caudate and putamen volumes in HD patients and smaller changes in the relative volumes of gray matter, white matter, and cerebrospinal fluid (Table 2). TFC scores in HD patients were correlated with caudate volume ($r = 0.72$, $P = 0.0002$), putamen volume ($r = 0.58$, $P = 0.009$), and relative gray-matter volume ($r = 0.50$, $P = 0.028$) and inversely correlated with relative cerebrospinal fluid volume ($r = −0.79$, $P = 6 \cdot 10^{-5}$). UHDRS motor scores in HD patients were correlated with relative cerebrospinal fluid volume ($r = 0.70$, $P = 0.0008$) and inversely correlated with caudate volume ($r = −0.66$, $P = 0.002$), putamen volume ($r = −0.50$, $P = 0.028$), and relative gray-matter volume ($r = −0.64$, $P = 0.003$). Disease

TABLE 1. Demographic and Clinical Characteristics of Subjects

Parameter	HD All (n = 20)	HD Early (n = 7)	Control (n = 14)
Sex (n)			
M	8	3	6
F	12	4	8
Age (y)	53.3 ± 12.1 (32.3–83.1)	47.3 ± 11.6 (32.3–64.5)	54.3 ± 12.9 (30.7–68.5)
Weight (kg)	65.9 ± 11.1 (50.0–89.0)*	71.7 ± 9.9 (60.0–89.0)	75.7 ± 10.6 (58.0–95.0)
$(CAG)_n$	43.6 ± 2.8 (39–50)	44.3 ± 3.9 (40–50)	—
Estimated disease duration (y)	6.0 ± 5.5 (0.5–19.4)	1.9 ± 1.5 (0.5–4.5)	—
UHDRS motor score	35.2 ± 25.0 (8–80)	15.0 ± 6.1 (8–27)	—
UHDRS TFC score	6.4 ± 4.8 (0–13)	11.9 ± 0.9 (11–13)	—
Shoulson–Fahn stage			—
I	7	7	
II	3	0	
III	4	0	
IV	4	0	
V	2	0	
Handedness			
L	2	0	3
Ambidexter	0	0	1
R	18	7	10

*Significant difference between patients and controls ($P < 0.05$).

Values represent mean ± SD, with range in parentheses. UHDRS motor scale ranges from 0 to 124, with higher scores indicating more motor impairment. UHDRS TFC scale assesses ability to perform daily activities and ranges from 13 (no impairment) to 0 (total incapacity). TFC scores are further subdivided into 5 Shoulson–Fahn stages: I (representing TFC scores 11–13), II (scores 7–10), III (scores 3–6), IV (scores 1–2), and V (score 0).

TABLE 2. Volumetric Cerebral and Striatal Data in HD Patients Versus Controls

Parameter	HD ($n = 19$)	Control ($n = 14$)
Gray-matter volume (relative to intracranial volume)	0.447 ± 0.031*	0.474 ± 0.018
White-matter volume (relative to intracranial volume)	0.248 ± 0.033	0.273 ± 0.016
Cerebrospinal fluid volume (relative to intracranial volume)	0.305 ± 0.041*	0.253 ± 0.019
Mean caudate volume[†] (cm^3)	1.13 ± 0.47[‡]	3.69 ± 0.35
Mean putamen volume[†] (cm^3)	1.54 ± 0.68[‡]	3.78 ± 0.55

*$P < 0.01$.
[†]Mean of left and right sides.
[‡]$P < 10^{-10}$ vs. controls.

burden (reflected by ($[CAG]_n - 35.5) \times age$), which has been shown to correlate with neuropathologic striatal damage (*14*), was inversely correlated to caudate volume ($r = -0.44$, $P = 0.05$). There was no significant correlation between these volumetric measures and $(CAG)_n$.

CB1 PET

Parametric images of partial-volume–corrected ^{18}F-MK9470 modified standardized uptake value, reflecting receptor availability (supplemental materials), showed a widespread decrease of CB1 in HD patients, compared with controls (Fig. 1). Statistical parametric mapping analysis showed highly significant reductions of CB1 availability in the HD group in all gray-matter regions at a cluster of P value of less than 0.0001 and familywise error–corrected height threshold of less than 0.05. When age, sex, and weight were explicitly taken as nuisance variables, group differences in statistical parametric mapping still showed similar results. Volume-of-interest–based statistical analysis showed that regional variation of the CB1 decrease in HD

was overall relatively small between gray-matter regions: reductions of CB1 availability ranged from approximately 15% in the cerebellum to approximately 25% in the frontal cortex (Fig. 2; Supplemental Table 1). No significant differences in white-matter signal were found between the 2 groups. Without partial-volume correction, similar reductions of CB1 availability were found in the HD group (Supplemental Table 1).

Importantly, the reduction of CB1 availability throughout the gray matter occurred early in the course of HD, as shown by analysis of the subgroup of 7 HD patients in the mildest stage of symptomatic disease (Figs. 1 and 2). Because a significant decrease of similar magnitude was found when only those HD patients ($n = 7$) who did not take any medication (data not shown) were included, the widespread reduction of CB1 availability was not due to medication use.

We found no correlations between CB1 availability and UHDRS motor scores, TFC scores, disease duration, or $(CAG)_n$. However, a modest inverse correlation was observed between CB1 availability and ($[CAG]_n - 35.5) \times age$ for a cluster in the frontal cortex (frontal volume of interest, $r = -0.49$, $P = 0.04$; Fig. 3). This correlation was most pronounced in the prefrontal cortex (frontopolar, Brodmann area 10, $r = -0.59$, $P = 0.010$) and premotor cortex (Brodmann area 6, $r = -0.50$, $P = 0.03$).

DISCUSSION

This study is the first, to our knowledge, in vivo demonstration of disturbance of the ECS in a human neurologic disease. The reduction of CB1 availability in the HD brain was profound and surprisingly widespread, affecting the entire gray matter of the cerebrum, brain stem, and cerebellum, even in the earliest symptomatic stage of the disease.

The widespread and relatively uniform reduction of CB1 availability throughout the gray matter in early HD contrasts with the regional selectivity of early disease changes detected in previous neuropathologic, MRI, and PET studies. Neuronal cell loss and huntingtin aggregates tend to be mostly confined to the striatum in early HD, whereas other brain areas show neuropathologic changes only in more advanced disease stages (*5*). Similarly, volumetric MRI in early HD detected atrophy of the striatum and parts of the cerebral cortex and hypothalamus, whereas volume loss was minimal
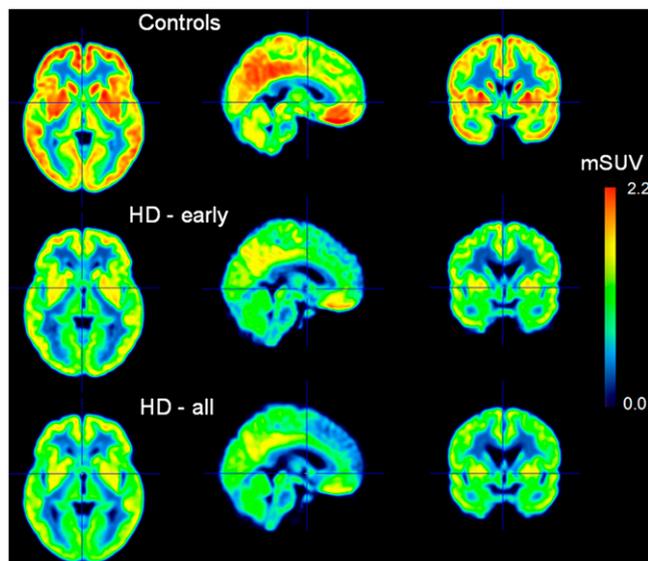
FIGURE 1. Cross-sectional, partial-volume corrected, modified standardized uptake value (mSUV) parametric images, averaged for all controls ($n = 14$), early-HD patients ($n = 7$), and total group of HD patients ($n = 19$).

FIGURE 2. Bar chart of regional differences in CB1 availability (^{18}F-MK-9470 binding) between HD and controls after partial-volume correction. ***$P < 0.001$ vs. controls. Mes temp = mesial temporal; mSUV = modified standardized uptake value; n.s. = not significant. Error bars indicate 1 SD.
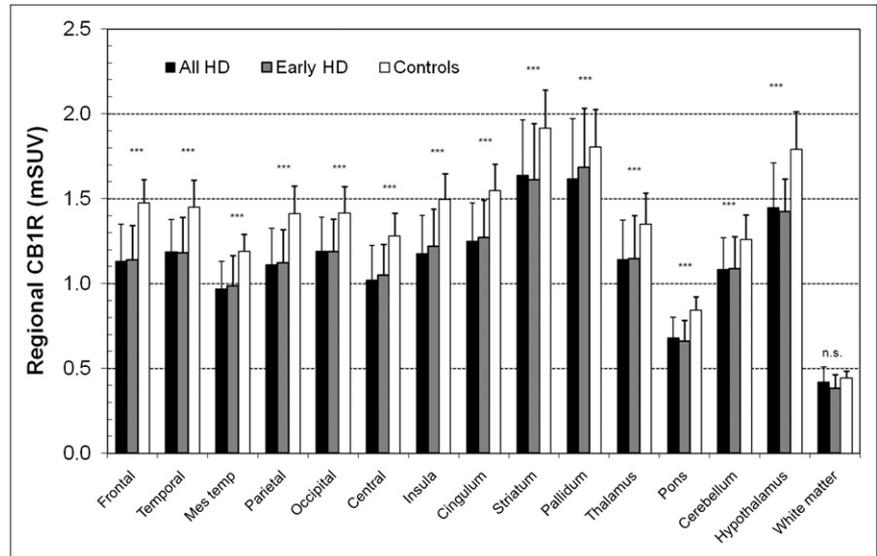
or undetectable in most other gray-matter regions such as the cerebellum (6,15). ^{18}F-FDG PET studies in early HD revealed significant reductions in glucose metabolism in the striatum and cerebral cortex but not elsewhere (16,17), and even in advanced stages, changes in glucose metabolism remained minimal in areas such as the cerebellum and thalamus (17,18). It is interesting to compare our CB1 PET results with PET studies that used tracers for other neuronal membrane receptors. Dopamine D_2 receptor binding is reduced in the striatum and regions of the cerebral cortex in HD (19,20),

but there have been no reports of studies with high-affinity D_2 receptor tracers that would allow a full assessment of changes in extrastriatal D_2 receptors. A PET study with the γ-amino-butyric acid A receptor tracer ^{11}C-flumazenil in 6 patients with early HD found a significant reduction of receptor density in the caudate but not in the cerebral cortex, thalamus, cerebellum, or pons (21). Finally, a study with the opioid receptor tracer ^{11}C-diprenorphine in 5 early-stage HD patients found tracer binding changes in the striatum, cingulate cortex, thalamus, and prefrontal cortex but not elsewhere (22). Data in these cited PET studies were not corrected for partial-volume effects and may have been confounded by regional volume loss.

The widespread distribution of the CB1 changes in HD fits well with the reported repressive effect of mutant huntingtin on CB1 transcription (9), given the ubiquitous expression pattern of mutant huntingtin and the transcription factors it interacts with (7). However, our findings could also be due to other contributing mechanisms such as increased degradation of CB1 mRNA or protein, impaired translation or trafficking, or changes in receptor affinity. Irrespective of the underlying mechanism, our findings strongly suggest that the ECS is hypoactive in HD. Given the crucial role of CB1 signaling in the regulation of neurotransmitter release, the reduction of CB1 levels would be expected to disturb synaptic transmission. It will be important to investigate the relationship between the CB1 changes and various cognitive and psychiatric symptoms of HD, especially because we found an inverse correlation between disease burden and CB1 availability in the prefrontal cortex. Intriguingly, a recent double-blind, placebo-controlled pilot study of nabilone, a CB1 agonist, in HD patients found evidence suggestive of neuropsychiatric improvement in the nabilone arm (23). Given the likely involvement of excitotoxicity in HD and the antiexcitotoxic effect of CB1 activation (24), the loss

FIGURE 3. Surface rendering of voxel-based correlation between absolute CB1 availability and disease burden ($[(CAG)_n - 35.5] \times$ age) at peak height threshold $P_{height} < 0.005$ (uncorrected). Clusters are overlaid on surface-rendered average image of HD patients.

of CB1 might also exacerbate neuronal injury in vulnerable brain regions.

There was a modest inverse correlation between disease burden and CB1 availability in the prefrontal and premotor cortex but not in other brain regions such as the striatum. The rather stable low-level CB1 availability in the striatum during symptomatic HD progression is reminiscent of transgenic HD mouse data showing that striatal CB1 mRNA declines in the presymptomatic phase but reaches a steady-state low level around the onset of overt symptoms. However, CB1 availability in the brain tends to increase with age in healthy humans, especially in women (*13*). Thus, the relative stability of CB1 availability in most brain regions during symptomatic HD progression represents a deviation from the pattern observed with healthy aging.

The profoundly decreased CB1 availability in patients with early symptomatic HD suggests that the decline in CB1 levels already begins in the presymptomatic phase of HD. Therefore, it will be important to track the evolution of CB1 levels in premanifest carriers of the HD mutation and determine whether CB1 PET could provide a biomarker for the earliest subclinical disease changes. It will be important to investigate whether administration of CB1 agonists, elevation of endocannabinoid levels, or delay of the loss of CB1—for instance, by providing a stimulating environment (*25*)—might be of benefit in the treatment of HD.

CONCLUSION

Our data show a widespread disturbance of the ECS in HD brains in vivo. Our findings suggest that some of the deleterious effects of mutant huntingtin may in fact be as ubiquitous as the expression of the mutant protein itself.

REFERENCES

1. Katona I, Freund TF. Endocannabinoid signaling as a synaptic circuit breaker in neurological disease. *Nat Med.* 2008;14:923–930.
2. Kreitzer AC, Malenka RC. Endocannabinoid-mediated rescue of striatal LTD and motor deficits in Parkinson's disease models. *Nature.* 2007;445:643–647.
3. Maldonado R, Valverde O, Berrendero F. Involvement of the endocannabinoid system in drug addiction. *Trends Neurosci.* 2006;29:225–232.
4. Walker FO. Huntington's disease. *Lancet.* 2007;369:218–228.
5. Vonsattel JP, DiFiglia M. Huntington disease. *J Neuropathol Exp Neurol.* 1998;57:369–384.
6. Kassubek J, Juengling FD, Kioschies T, et al. Topography of cerebral atrophy in early Huntington's disease: a voxel based morphometric MRI study. *J Neurol Neurosurg Psychiatry.* 2004;75:213–220.
7. Dunah AW, Jeong H, Griffin A, et al. Sp1 and TAFII130 transcriptional activity disrupted in early Huntington's disease. *Science.* 2002;296:2238–2243.
8. Butler R, Bates GP. Histone deacetylase inhibitors as therapeutics for polyglutamine disorders. *Nat Rev Neurosci.* 2006;7:784–796.
9. Kuhn A, Goldstein DR, Hodges A, et al. Mutant huntingtin's effects on striatal gene expression in mice recapitulate changes observed in human Huntington's disease brain and do not differ with mutant huntingtin length or wild-type huntingtin dosage. *Hum Mol Genet.* 2007;16:1845–1861.
10. Glass M, Dragunow M, Faull RL. The pattern of neurodegeneration in Huntington's disease: a comparative study of cannabinoid, dopamine, adenosine and GABA$_A$ receptor alterations in the human basal ganglia in Huntington's disease. *Neuroscience.* 2000;97:505–519.
11. Burns HD, Van Laere K, Sanabria-Bohorquez S, et al. [^{18}F]MK-9470, a positron emission tomography (PET) tracer for in vivo human PET brain imaging of the cannabinoid-1 receptor. *Proc Natl Acad Sci USA.* 2007;104:9800–9805.
12. Huntington Study Group. Unified Huntington's Disease Rating Scale: reliability and consistency. *Mov Disord.* 1996;11:136–142.
13. Van Laere K, Goffin K, Casteels C, et al. Gender-dependent increases with healthy aging of the human cerebral cannabinoid-type 1 receptor binding using [^{18}F]MK-9470 PET. *Neuroimage.* 2008;39:1533–1541.
14. Penney JB Jr, Vonsattel JP, MacDonald ME, Gusella JF, Myers RH. CAG repeat number governs the development rate of pathology in Huntington's disease. *Ann Neurol.* 1997;41:689–692.
15. Rosas HD, Koroshetz WJ, Chen YI, et al. Evidence for more widespread cerebral pathology in early HD: an MRI-based morphometric analysis. *Neurology.* 2003;60:1615–1620.
16. Hayden MR, Martin WR, Stoessl AJ, et al. Positron emission tomography in the early diagnosis of Huntington's disease. *Neurology.* 1986;36:888–894.
17. Martin WR, Clark C, Ammann W, Stoessl AJ, Shtybel W, Hayden MR. Cortical glucose metabolism in Huntington's disease. *Neurology.* 1992;42:223–229.
18. Kuwert T, Lange HW, Langen KJ, Herzog H, Aulich A, Feinendegen LE. Cortical and subcortical glucose consumption measured by PET in patients with Huntington's disease. *Brain.* 1990;113:1405–1423.
19. Pavese N, Andrews TC, Brooks DJ, et al. Progressive striatal and cortical dopamine receptor dysfunction in Huntington's disease: a PET study. *Brain.* 2003;126:1127–1135.
20. Antonini A, Leenders KL, Spiegel R, et al. Striatal glucose metabolism and dopamine D2 receptor binding in asymptomatic gene carriers and patients with Huntington's disease. *Brain.* 1996;119:2085–2095.
21. Holthoff VA, Koeppe RA, Frey KA, et al. Positron emission tomography measures of benzodiazepine receptors in Huntington's disease. *Ann Neurol.* 1993;34:76–81.
22. Weeks RA, Cunningham VJ, Piccini P, Waters S, Harding AE, Brooks DJ. ^{11}C-diprenorphine binding in Huntington's disease: a comparison of region of interest analysis with statistical parametric mapping. *J Cereb Blood Flow Metab.* 1997;17:943–949.
23. Curtis A, Mitchell I, Patel S, Ives N, Rickards H. A pilot study using nabilone for symptomatic treatment in Huntington's disease. *Mov Disord.* 2009;24:2254–2259.
24. Marsicano G, Goodenough S, Monory K, et al. CB1 cannabinoid receptors and on-demand defense against excitotoxicity. *Science.* 2003;302:84–88.
25. Glass M, van Dellen A, Blakemore C, Hannan AJ, Faull RL. Delayed onset of Huntington's disease in mice in an enriched environment correlates with delayed loss of cannabinoid CB1 receptors. *Neuroscience.* 2004;123:207–212.